SANDIA REPORT

SAND2008-2262

Unlimited Release

Printed May 2008

Hybrid Method for the Precise Calculation of the General Dyadic Greens Functions for SAW and Leaky Wave Substrates

Darren W. Branch

Prepared by
Sandia National Laboratories
Albuquerque, New Mexico 87185 and Livermore, California 94550

Sandia is a multiprogram laboratory operated by Sandia Corporation,
a Lockheed Martin Company, for the United States Department of Energy's
National Nuclear Security Administration under Contract DE-AC04-94AL85000.

Approved for public release; further dissemination unlimited.

Sandia National Laboratories

Issued by Sandia National Laboratories, operated for the United States Department of Energy by Sandia Corporation.

NOTICE: This report was prepared as an account of work sponsored by an agency of the United States Government. Neither the United States Government, nor any agency thereof, nor any of their employees, nor any of their contractors, subcontractors, or their employees, make any warranty, express or implied, or assume any legal liability or responsibility for the accuracy, completeness, or usefulness of any information, apparatus, product, or process disclosed, or represent that its use would not infringe privately owned rights. Reference herein to any specific commercial product, process, or service by trade name, trademark, manufacturer, or otherwise, does not necessarily constitute or imply its endorsement, recommendation, or favoring by the United States Government, any agency thereof, or any of their contractors or subcontractors. The views and opinions expressed herein do not necessarily state or reflect those of the United States Government, any agency thereof, or any of their contractors.

Printed in the United States of America. This report has been reproduced directly from the best available copy.

Available to DOE and DOE contractors from
U.S. Department of Energy
Office of Scientific and Technical Information
P.O. Box 62
Oak Ridge, TN 37831

Telephone: (865)576-8401
Facsimile: (865)576-5728
E-Mail: reports@adonis.osti.gov
Online ordering: http://www.osti.gov/bridge

Available to the public from
U.S. Department of Commerce
National Technical Information Service
5285 Port Royal Rd
Springfield, VA 22161

Telephone: (800)553-6847
Facsimile: (703)605-6900
E-Mail: orders@ntis.fedworld.gov
Online order: http://www.ntis.gov/help/ordermethods.asp?loc=7-4-0#online

SAND2008-2262

Unlimited Release

Printed May 2008

Hybrid Method for the Precise Calculation of the General Dyadic Greens Functions for SAW and Leaky Wave Substrates

Darren W. Branch

Biosensors and Nanomaterials Department
Sandia National Laboratories
PO Box 5800
Albuquerque, NM 87185-1425

ABSTRACT

Recently, the generalized method for calculation of the 16-element Green's function for analysis of surface acoustic waves has proven crucial to develop more sophisticated transducers. The generalized Green's function provides a precise relationship between the acoustic stresses and electric displacement on the three mechanical displacements and electric potential. This generalized method is able to account for mass loading effects which is absent in the effective permittivity approach. However, the calculation is numerically intensive and may lead to numerical instabilities when solving for both the eigenvalues and eigenvectors simultaneously. In this work, the general eigenvalue problem was modified to eliminate the numerical instabilities in the solving procedure. An algorithm is also presented to select the proper eigenvalues rapidly to facilitate analysis for all types of acoustic propagation. The 4x4 Green's functions and effective permittivities were calculated for materials supporting Rayleigh, leaky, and leaky longitudinal waves as demonstration of the method.

TABLE OF CONTENTS

Abstract 3

I. Introduction 7

II. Theory 8

A. Traditional Method 9

Boundary Conditions *11*

B. Generalized Method 13

C. Hybrid Method 14

III. Algorithms and Solving Procedure 15

A. Crystal Rotation 15

B. Cut-off Velocities 16

C. Root Selection 17

D. Effective Permittivity 18

IV. Results 19

A. 128° YX Lithium Niobate (Rayleigh Waves) 19

B. 36° YX Lithium Tantalate (SH Leaky Waves) 24

C. 47.3° Y 90° X off-axis Lithium Tetraborate (Longitudinal Leaky Waves) 27

D. Effective Permittivity for 128º YX LNBO (SAW) 30

E. Effective Permittivity for 36º YX LTO (LSAW) 31

F. Effective Permittivity for 47.3° Y 90° X off-axis Lithium Tetraborate (LLSAW) 33

Conclusions 34

References 35

Distribution List 35

I. INTRODUCTION

The design and optimization of complex interdigital transducers on a wide variety of substrates requires detailed knowledge of wave excitation and propagation. The concept of the effective permittivity introduced the idea that a specific relationship exists between the charge and the electrical potential distribution [1]. To determine the amplitude of the electric potential, the full system of piezoelectric coupled acoustic and electrostatic equations must be solved. Due to linearity of elastic media, the amplitudes of the charge and potential are fortunately proportional to each other and their ratio is independent. In the absence of piezoelectricity, the effective permittivity reduces to the dielectric permittivity. The effective permittivity calculation takes into account generation of all possible acoustic waves propagating in the sagittal plane, excited by a charge distribution on a mechanically free surface. However, the limitation is that the effective permittivity does not address the relationship between surface stresses and charge on mechanical motion and acoustic potential. Instead, the complete description requires introduction of the 16-element Green's function, where the effective permittivity is represented by a single matrix element, G_{44}.

Calculation of the 16-element Green's function requires the use of matrix methods to change the problem from several independent steps involving determinants [2] and boundary condition matrices into a single compact eigenvalue problem [3] [4]. Once calculated, the Green's function provides a precise relationship between the acoustic stresses and electric displacement on the three mechanical displacement and electric potential. In this way, the Green's function acts as a source term for acoustic wave generation. The behavior is often highly complicated with no functional form which also depends on the type of excitation (e.g. Rayleigh). Once computed, interpolation methods can be used to capture the functional behavior by numerically sampling near the pole regions. Extending this technique permits calculation of a spatial Green's function, which can be very powerful toward analyzing acoustic wave excitation and propagation in interdigital structures [5].

This work focuses on the calculation of the 4x4 Green's function by re-formulating the eigenvalue problem to improve the accuracy of the eigenvalue calculation. Although the

general method provides both the eigenvalues and eigenvectors, the result is often numerically unstable. Instead, this approach determines the eigenvalues separately using the traditional method then computes each eigenvector by redefining the general eigenvalue problem. In addition, an algorithm was implemented to select the proper eigenvalues for any acoustic wave.

II. THEORY

Acoustic waves must satisfy both Newton's and Maxwell's equations. In the absence of external forces, the equations are expressed as

$$\rho \frac{\partial^2 u_i}{\partial t^2} = \nabla \cdot T \tag{1.1}$$

$$S = \nabla_s u \tag{1.2}$$

$$\nabla \cdot D = \rho_f \tag{1.3}$$

where is the mass density, u is the particle displacement, and T and S are the surface stress and strain components, respectively. D and $_f$ are the electric displacement and free charge density, respectively. The free charge density $_f$ is zero everywhere except at the surface of the substrate.

In a piezoelectric substrate, the coupled constitutive equations for piezoelectric media are given by:

$$T_{ij} = c^E_{ijkl} S_{kl} - e^t_{kij} E_k \tag{1.4}$$

$$D_i = e_{ikl} S_{kl} + \varepsilon^S_{ik} E_k \tag{1.5}$$

where e and c^E are the piezoelectric stress constants and stiffness constants. Since the coupling between the electric and elastic fields is weak, the magnetic fields can be neglected and the electric fields derived from the scalar potential. This is known as the static field approximation in which the particle displacements u_i are along the coordinate axis x_i. In (1.4) and (1.5), we recognize Hooke's law and $D = \varepsilon E$, where $E = -\nabla\phi$ and ϕ is the electrical potential on the surface. By substituting (1.4) and (1.5) into (1.1) and (1.3) yields,

$$\rho \frac{\partial^2 u}{\partial t^2} = \nabla \cdot c^E : \nabla_s u - \nabla \cdot \left(e \cdot E \right) \tag{1.6}$$

$$\nabla \cdot \left(e : \nabla_s u \right) - \nabla \cdot \left(\varepsilon^s \cdot \nabla \phi \right) = 0 \tag{1.7}$$

A. Traditional Method

To obtain solutions, plane wave forms are assumed for both the particle displacement and electric potential with the following forms for the piezoelectric substrate [2, 6-8],

$$\begin{aligned} u_i &= \left\{ \sum_{m=1}^{4} C_m \beta_i^m e^{\alpha^{(m)} k x_3} \right\} e^{j\omega\left(t - \frac{x_1}{v}\right)}, x_3 < 0 \\ \phi &= \left\{ \sum_{m=1}^{4} C_m \beta_4^m e^{\alpha^{(m)} k x_3} \right\} e^{j\omega\left(t - \frac{x_1}{v}\right)}, x_3 < 0 \end{aligned} \tag{1.8}$$

The trial solutions in (1.8) vary amongst authors [2, 6, 7] which changes the conditions for the allowed values of , otherwise the solution process is identical. Substituting (1.8) into (1.6) and (1.7), gives four linear equations for particle displacement u and potential ϕ [9]

$$A \begin{bmatrix} \overline{u_1} \\ \overline{u_2} \\ \overline{u_3} \\ \overline{\phi} \end{bmatrix} = \left(\alpha^2 A_1 - j\alpha A_2 + A_3 \right) \begin{bmatrix} \overline{u_1} \\ \overline{u_2} \\ \overline{u_3} \\ \overline{\phi} \end{bmatrix} = 0 \tag{1.9}$$

where A is a second order function of , and the bars indicate the Fourier transformation with respect to x_1 in k-space. The coefficients of the matrix are given as

$$A_1 = \begin{bmatrix} c_{55}^E & c_{45}^E & c_{35}^E & e_{35} \\ c_{45}^E & c_{44}^E & c_{34}^E & e_{34} \\ c_{35}^E & c_{34}^E & c_{33}^E & e_{33} \\ e_{35} & e_{34} & e_{33} & -\varepsilon_{33}^S \end{bmatrix} \tag{1.10}$$

$$A_2 = \begin{bmatrix} c_{15}^E + c_{51}^E & c_{14}^E + c_{56}^E & c_{13}^E + c_{55}^E & e_{15}^E + e_{31} \\ c_{14}^E + c_{56}^E & c_{46}^E + c_{64}^E & c_{36}^E + c_{45}^E & e_{14}^E + e_{36} \\ c_{13}^E + c_{55}^E & c_{36}^E + c_{45}^E & c_{35}^E + c_{53}^E & e_{13}^E + e_{35} \\ e_{15}^E + e_{31} & e_{14}^E + e_{36} & e_{13}^E + e_{35} & -\varepsilon_{13}^S - \varepsilon_{31}^S \end{bmatrix} \tag{1.11}$$

$$A_3 = \begin{bmatrix} -c_{11}^E + \rho v^2 & -c_{16}^E & -c_{15}^E & -e_{11} \\ -c_{16}^E & -c_{66}^E + \rho v^2 & -c_{56}^E & -e_{16} \\ -c_{15}^E & -c_{56}^E & -c_{55}^E + \rho v^2 & -e_{15} \\ -e_{11} & -e_{16} & -e_{15} & \varepsilon_{11} \end{bmatrix} \tag{1.12}$$

where $v = \omega / k$ is the phase velocity along the x_1 direction. For non-trivial solution of (1.9) the determinant of the coefficient matrix A must be zero for each value of , which leads to an 8th order polynomial in . Bounded solutions in (1.8) further require the $\mathrm{Re}\left\{k\alpha^{(m)}\right\} > 0$ to eliminate solutions that increase with depth into the substrate. For each valid root $\alpha^{(m)}$, we obtain four eigenvectors $\beta_i^{(m)} \to \beta_1^1, \beta_2^1, \beta_3^1, \beta_4^1$ and thus a partial wave solution. The solution of the system of linear equations is a linear combination of these partial solutions normalized by ϕ given as

$$\begin{bmatrix} \overline{u_1} \\ \overline{u_2} \\ \overline{u_3} \\ \overline{\phi} \end{bmatrix} = \begin{bmatrix} \beta_1^{(1)} & \beta_1^{(2)} & \beta_1^{(3)} & \beta_1^{(4)} \\ \beta_2^{(1)} & \beta_2^{(2)} & \beta_2^{(3)} & \beta_2^{(4)} \\ \beta_3^{(1)} & \beta_3^{(2)} & \beta_3^{(3)} & \beta_3^{(4)} \\ 1 & 1 & 1 & 1 \end{bmatrix} \begin{bmatrix} C_1 e^{\alpha^{(1)} k x_3} \\ C_2 e^{\alpha^{(2)} k x_3} \\ C_3 e^{\alpha^{(3)} k x_3} \\ C_4 e^{\alpha^{(4)} k x_3} \end{bmatrix} \tag{1.13}$$

The stresses and electrical displacement are obtained by substituting (1.13) into (1.4) and (1.5)

$$\begin{bmatrix} \overline{T_{13}} \\ \overline{T_{23}} \\ \overline{T_{33}} \\ \overline{D_3} \end{bmatrix} = \begin{bmatrix} \overline{T_{13}^{(1)}} & \overline{T_{13}^{(2)}} & \overline{T_{13}^{(3)}} & \overline{T_{13}^{(4)}} \\ \overline{T_{23}^{(1)}} & \overline{T_{23}^{(2)}} & \overline{T_{23}^{(3)}} & \overline{T_{23}^{(4)}} \\ \overline{T_{33}^{(1)}} & \overline{T_{33}^{(2)}} & \overline{T_{33}^{(3)}} & \overline{T_{33}^{(4)}} \\ \overline{D_3^{(1)}} & \overline{D_3^{(2)}} & \overline{D_3^{(3)}} & \overline{D_3^{(4)}} \end{bmatrix} \begin{bmatrix} C_1 e^{\alpha^{(1)} k x_3} \\ C_2 e^{\alpha^{(2)} k x_3} \\ C_3 e^{\alpha^{(3)} k x_3} \\ C_4 e^{\alpha^{(4)} k x_3} \end{bmatrix} \tag{1.14}$$

where

$$\begin{bmatrix} \overline{T_{13}^{(i)}} \\ \overline{T_{23}^{(i)}} \\ \overline{T_{33}^{(i)}} \\ \overline{D_3^{(i)}} \end{bmatrix} = k\left(\alpha^{(i)} A_1 - jA_4\right) \begin{bmatrix} \overline{u_1^{(i)}} \\ \overline{u_2^{(i)}} \\ \overline{u_3^{(i)}} \\ 1 \end{bmatrix}, i \to 1...4 \tag{1.15}$$

$$A_4 = \begin{bmatrix} c_{15}^E & c_{56}^E & c_{55}^E & e_{15} \\ c_{14}^E & c_{46}^E & c_{45}^E & e_{14} \\ c_{13}^E & c_{36}^E & c_{35}^E & e_{13} \\ e_{31} & e_{36} & e_{35} & -\varepsilon_{13}^s \end{bmatrix} \tag{1.16}$$

Boundary Conditions

The coefficients C_m are determined from application of the boundary conditions, requiring stress free conditions at the free surface $x_3 = 0$,

$$T_{13}\left(x_1, 0\right) = T_{23}\left(x_1, 0\right) = T_{33}\left(x_1, 0\right) = 0 \tag{1.17}$$

Additional layers require continuity of stresses and displacement with 12 boundary conditions per for piezoelectric layers. For the electric displacement D the normal component must be continuous across the boundary at x_3=0. Inside the piezoelectric substrate the electric displacement is given by

$$D_3\left(x_1, 0^-\right) = e_{3kl} \frac{\partial u_k}{\partial x_l} - \varepsilon_{3k} \frac{\partial \phi}{\partial x_k} \tag{1.18}$$

In the vacuum above the substrate (x_3> 0), the electrical potential must satisfy Laplace's equation

$$\nabla^2 \phi = \frac{\partial^2 \phi}{\partial x_1^2} + \frac{\partial^2 \phi}{\partial x_3^2} = 0 \tag{1.19}$$

Because ϕ is proportional to e^{-jkx_1} and must vanish at $x_3 \to \infty$, the x_3 dependence is $e^{-|k|x_3}$ for x_3 > 0. For each solution of $\alpha^{(m)}$, there is one corresponding partial wave solution of the potential for x_3 > 0, and the potential must be continuous across the free surface giving,

$$\phi\left(x_1, x_3 > 0\right) = \sum_{m=1}^{4} C_m e^{-jkx_1 - |k| x_3} \tag{1.20}$$

Therefore,

$$D_3\left(x_1, 0^+\right) = -\varepsilon_0 \frac{\partial \phi}{\partial x_3} = \varepsilon_0 k \sum_{m=1}^{4} C_m e^{-jkx_1} \tag{1.21}$$

The electrical boundary condition at $x_3=0$ surface is

$$D_3\left(x_1, 0^+\right) - D_3\left(x_1, 0^-\right) = \sigma\left(x_1\right) \tag{1.22}$$

where is the surface charge density. The surface potential $\phi\left(x_1, 0\right)$ must be the same on both sides of the boundary however the normal components of the electrical displacement can differ. The discontinuity is related to the potential by the effective permittivity $\varepsilon_s\left(k\right)$ as

$$\varepsilon_s\left(k\right) = \frac{\overline{D_3}\left(k\right)\Big|_{x_3=0^+} - \overline{D_3}\left(k\right)\Big|_{x_3=0^-}}{|k| \cdot \overline{\phi}\left(k\right)} = \frac{\overline{\sigma}\left(k\right)}{|k| \cdot \overline{\phi}\left(k\right)} \tag{1.23}$$

The Green's function is defined as the potential excited by a line source with free charge density, such that

$$\phi\left(x_1, 0\right) = G_{44}\left(x_1, 0\right) * \sigma\left(x_1, 0\right) \tag{1.24}$$

In the absence of surface stresses, this expression fully describes the behavior of acoustic waves when the electrical boundary conditions are applied. The two electrical conditions considered are zero charge on un-metallized surface regions (open-condition) and constant potential on metallized surface regions (short-condition). Applying the Fourier transformation with respect to x_1 on both sides of (1.24) gives an expression in the k domain,

$$\overline{G_{44}}\left(k\right) = \frac{\overline{\phi}\left(k\right)}{\overline{\sigma}\left(k\right)} \tag{1.25}$$

Therefore the effective permittivity can be determined using,

$$\varepsilon_s(k) = \frac{\overline{\sigma}(k)}{|k|\overline{\phi}(k)} = \frac{1}{k \cdot \overline{G_{44}}(k)} \tag{1.26}$$

B. Generalized Method

In the general Green's function approach the vector $\begin{bmatrix} \overline{T_{13}} & \overline{T_{23}} & \overline{T_{33}} & \overline{D_3'} \end{bmatrix}$ is defined as the exciting source. The Green's function can be expressed as

$$\overline{G} = \begin{bmatrix} \beta_1^{(1)} & \beta_1^{(2)} & \beta_1^{(3)} & \beta_1^{(4)} \\ \beta_2^{(1)} & \beta_2^{(2)} & \beta_2^{(3)} & \beta_2^{(4)} \\ \beta_3^{(1)} & \beta_3^{(2)} & \beta_3^{(3)} & \beta_3^{(4)} \\ 1 & 1 & 1 & 1 \end{bmatrix} \begin{bmatrix} C_1 \\ C_2 \\ C_3 \\ C_4 \end{bmatrix} \begin{bmatrix} \overline{T_{13}^{(1)}} & \overline{T_{13}^{(2)}} & \overline{T_{13}^{(3)}} & \overline{T_{13}^{(4)}} \\ \overline{T_{23}^{(1)}} & \overline{T_{23}^{(2)}} & \overline{T_{23}^{(3)}} & \overline{T_{23}^{(4)}} \\ \overline{T_{33}^{(1)}} & \overline{T_{33}^{(2)}} & \overline{T_{33}^{(3)}} & \overline{T_{33}^{(4)}} \\ \overline{D_3^{(1)\prime}} & \overline{D_3^{(2)\prime}} & \overline{D_3^{(3)\prime}} & \overline{D_3^{(4)\prime}} \end{bmatrix}^{-1} \Bigg|_{x_3=0} \tag{1.27}$$

Setting $\overline{u_i}(x_3 = 0) = \sum_{m=1}^{4} C_m \beta_i^m, i \to 1...4$ gives

$$\overline{G} = \begin{bmatrix} \overline{u_1^{(1)}} & \overline{u_1^{(2)}} & \overline{u_1^{(3)}} & \overline{u_1^{(4)}} \\ \overline{u_2^{(1)}} & \overline{u_2^{(2)}} & \overline{u_2^{(3)}} & \overline{u_2^{(4)}} \\ \overline{u_3^{(1)}} & \overline{u_3^{(2)}} & \overline{u_3^{(3)}} & \overline{u_3^{(4)}} \\ 1 & 1 & 1 & 1 \end{bmatrix} \begin{bmatrix} \overline{T_{13}^{(1)}} & \overline{T_{13}^{(2)}} & \overline{T_{13}^{(3)}} & \overline{T_{13}^{(4)}} \\ \overline{T_{23}^{(1)}} & \overline{T_{23}^{(2)}} & \overline{T_{23}^{(3)}} & \overline{T_{23}^{(4)}} \\ \overline{T_{33}^{(1)}} & \overline{T_{33}^{(2)}} & \overline{T_{33}^{(3)}} & \overline{T_{33}^{(4)}} \\ \overline{D_3^{(1)\prime}} & \overline{D_3^{(2)\prime}} & \overline{D_3^{(3)\prime}} & \overline{D_3^{(4)\prime}} \end{bmatrix}^{-1} \tag{1.28}$$

and $\overline{D_3^{(i)\prime}} = \overline{D_3^{(i)}}(0^+) - \overline{D_3^{(i)}}(0^-) = \varepsilon_o k - \overline{D_3^{(i)}}(0^-)$. The shorted condition at the boundary requires $D_3(x_1, 0^+) = 0$ or $\overline{D_3^{(i)\prime}} = \overline{D_3^{(i)}}(0^-)$. To facilitate calculation of the Green's function, the eigenvalue problem in (1.9) and (1.15) is written as

$$\left(\alpha^2 A_1 - j\alpha A_2 + A_3\right) \begin{Bmatrix} \overline{u} \\ \overline{\phi} \end{Bmatrix} = 0 \tag{1.29}$$

and

$$\frac{1}{k} \begin{Bmatrix} \overline{T} \\ \overline{D} \end{Bmatrix} = \left(\alpha A_1 - jA_4\right) \begin{Bmatrix} \overline{u} \\ \overline{\phi} \end{Bmatrix} \to \alpha A_1 \begin{Bmatrix} \overline{u} \\ \overline{\phi} \end{Bmatrix} = \frac{1}{k} \begin{Bmatrix} \overline{T} \\ \overline{D} \end{Bmatrix} + jA_4 \begin{Bmatrix} \overline{u} \\ \overline{\phi} \end{Bmatrix} \tag{1.30}$$

Substitution of (1.30) into (1.29) gives

$$\alpha\left[\frac{1}{k}\left\{\frac{\overline{T}}{\overline{D}}\right\}+jA_4\left\{\frac{\overline{u}}{\overline{\phi}}\right\}\right]-j\alpha A_2\left\{\frac{\overline{u}}{\overline{\phi}}\right\}+A_3\left\{\frac{\overline{u}}{\overline{\phi}}\right\}=0\rightarrow\alpha\frac{1}{k}\left\{\frac{\overline{T}}{\overline{D}}\right\}+j\alpha\left(A_4-A_2\right)\left\{\frac{\overline{u}}{\overline{\phi}}\right\}=-A_3\left\{\frac{\overline{u}}{\overline{\phi}}\right\} \quad (1.31)$$

Combining (1.31) with (1.30) yields the new eigenvalue problem,

$$\alpha\left[\begin{array}{c|c} 1 & j\left(A_4-A_2\right) \\ \hline 0 & A_1 \end{array}\right]\begin{bmatrix} T_{13}/k \\ T_{23}/k \\ T_{33}/k \\ D_3/k \\ u_1 \\ u_2 \\ u_3 \\ \phi \end{bmatrix}=\left[\begin{array}{c|c} 0 & -A_3 \\ \hline 1 & jA_4 \end{array}\right]\begin{bmatrix} T_{13}/k \\ T_{23}/k \\ T_{33}/k \\ D_3/k \\ u_1 \\ u_2 \\ u_3 \\ \phi \end{bmatrix} \quad (1.32)$$

As stated by Qiao et. al [9] equation (1.32) is a standard eigenvalue problem of the form $\alpha Bx = Ax$ that yields the eigenvalues and their corresponding eigenvectors together. In contrast, the traditional method determines the eigenvalues $\alpha^{(m)}$ first; then uses them to obtain the four corresponding eigenvectors in a piecewise fashion.

C. Hybrid Method

In this method calculating the Green's function uses a mixture of both methods to eliminate numerical instabilities in the generalized method while obtaining a high degree of precision in the solution. Since the numerical magnitude ranges from10^{12} to 10^{-12} for the values in (1.32), even the most robust eigenvalue solver has great difficulties. First equation (1.9) is solved for the eight values of $\alpha^{(m)}$ then four are selected for the appropriate propagating mode. Each eigenvalue is substituted into (1.32) yielding,

$$\alpha^{(m)}Bx = Ax \rightarrow \left(\alpha^{(m)}B - A\right)x = 0, \rightarrow Qx = 0, m = 1...4 \quad (1.33)$$

where

$$B = \left[\begin{array}{c|c} 1 & j\left(A_4 - A_2\right) \\ \hline 0 & A_1 \end{array}\right] \tag{1.34}$$

$$A = \left[\begin{array}{c|c} 0 & -A_3 \\ \hline 1 & jA_4 \end{array}\right] \tag{1.35}$$

Each eigenvalue $\alpha^{(m)}$ allows row-reduction of Q to determine the null basis for (1.33), in which are eight element column vectors comprising $\left[\overline{T} \quad \overline{D} \quad \overline{u} \quad \overline{\phi}\right]$. This approach obtains the precision of the traditional method, while using the general method to solve the entire problem without computing C_m explicitly from the boundary matrix.

III. Algorithms and Solving Procedure

A. Crystal Rotation

The crystal axis is chosen with x_3 normal to the crystal surface and x_1 is in the direction of propagation. The rotation procedure considers arbitrary orientations of the crystal with respect to the axis.

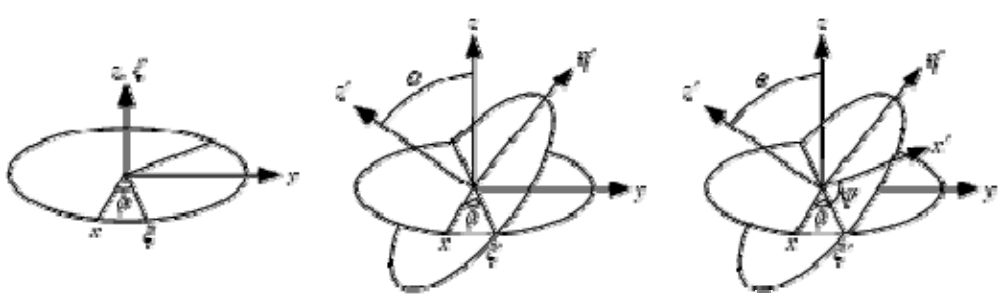

Fig. 1 Rotations for Euler angle definitions.

The rotation is performed by a coordinate rotation through application of the Euler angles (ϕ,θ,ψ) as defined by the matrices,

$$V_1 = \begin{bmatrix} \cos(\phi) & \sin(\phi) & 0 \\ -\sin(\phi) & \cos(\phi) & 0 \\ 0 & 0 & 1 \end{bmatrix}$$
$$V_2 = \begin{bmatrix} 1 & 0 & 0 \\ 0 & \cos(\theta) & \sin(\theta) \\ 0 & -\sin(\theta) & \cos(\theta) \end{bmatrix} \tag{1.36}$$
$$V_3 = \begin{bmatrix} \cos(\psi) & \sin(\psi) & 0 \\ -\sin(\psi) & \cos(\psi) & 0 \\ 0 & 0 & 1 \end{bmatrix}$$

This is termed the "x-convention," which is the most common definition [10]. In this convention, the rotation given by Euler angles (ϕ,θ,ψ) has the first rotation by angle ϕ about the *z*-axis, the second by angle θ about the *x*-axis and the third by angle ψ about the *z*-axis. The stiffness, piezoelectric, and permittivity tensors are rotated using,

$$a = V_3 \cdot V_2 \cdot V_1 \tag{1.37}$$

$$M = \begin{bmatrix} a_{11}^2 & a_{12}^2 & a_{13}^2 & 2a_{12}a_{13} & 2a_{11}a_{13} & 2a_{11}a_{12} \\ a_{21}^2 & a_{22}^2 & a_{23}^2 & 2a_{22}a_{23} & 2a_{21}a_{23} & 2a_{21}a_{22} \\ a_{31}^2 & a_{32}^2 & a_{33}^2 & 2a_{32}a_{33} & 2a_{33}a_{31} & 2a_{31}a_{32} \\ 2a_{21}a_{31} & 2a_{22}a_{32} & 2a_{23}a_{33} & a_{22}a_{33}+a_{23}a_{32} & a_{21}a_{33}+a_{23}a_{31} & a_{22}a_{31}+a_{21}a_{32} \\ 2a_{11}a_{31} & 2a_{32}a_{12} & 2a_{13}a_{33} & a_{12}a_{33}+a_{13}a_{32} & a_{13}a_{31}+a_{11}a_{33} & a_{11}a_{32}+a_{12}a_{31} \\ 2a_{11}a_{21} & 2a_{12}a_{22} & 2a_{13}a_{23} & a_{12}a_{23}+a_{13}a_{22} & a_{13}a_{21}+a_{11}a_{23} & a_{11}a_{22}+a_{12}a_{21} \end{bmatrix} \tag{1.38}$$

$$C' = M \cdot C \cdot M^T$$
$$e' = a \cdot e \cdot M^T \tag{1.39}$$
$$\varepsilon' = a \cdot \varepsilon \cdot a^T$$

B. Cut-off Velocities

The cut-off velocities are the values where the eigenvalue modes change as the velocity, *v* is varied. By solving (1.12) for *v*, up to three unique values can be

determined. For a particular crystals and rotation, degeneracy's reduce the number of unique cut-off points. The significance of the cut-off points is that they determine where the propagating acoustic mode changes from Rayleigh to the leaky types. For a Rayleigh wave, there exists four eigenvalues decaying beneath the surface [2], and waves with three eigenvalues decaying beneath with a bulk wave radiating into the solid are called leaky surface waves [11]. Leaky longitudinal waves consist of two bulk shear waves radiating into the solid, a longitudinal wave, and an electromagnetic wave propagating along the surface decaying into the depth [12].

$$\begin{aligned} &v < v_{s1} : Rayleigh\ \ Wave \\ &v_{s1} < v < v_{s2} : Bulk,\ \ Leaky\ \ Wave \\ &v_{s2} < v < v_{l} : Leaky\ Longitudinal\ Wave \end{aligned} \tag{1.40}$$

Expression (1.12) is an incomplete eigenvalue problem, where the eigenvalue ρv^2 does not appear completely along the diagonal. Two methods are suitable for solving for the cut-off velocities. Symbolic expansion of the determinant yields a very large expression that can be solved for , however the method is slower since the evaluation time is larger, and the complete problem requires solving (1.9) for any given *v*. The second method redefines the eigenvalue problem by solving for the modified characteristic polynomial numerically and then building an equivalent matrix such that a standard solver can be called.

The computed matrices (1.10), (1.11), and (1.12) provide a convenient method to assess the coupling for a particular crystal and orientation. The algorithm first assumes that the problem is fully coupled then tests for coupling conditions. This procedure leads to the following conditions: 1) piezoelectricity decoupled with u_1 and u_3, 2) piezoelectricity decoupled with u_2, or 3) piezoelectricity fully decoupled with the acoustic fields.

C. Root Selection

The root selection criteria require that only four allowed values are selected from the eight values of for a given value of velocity. The selection is critical since the values of determine the decay behavior of the acoustic fields. As velocity is swept, the

behavior of changes such that the selection procedure must account for more terms decaying into the depth of the substrate. The proper roots are selected according to

$$\mathrm{Re}\left\{k\alpha^{(m)}\right\} > 0 \tag{1.41}$$

Many authors often use a specific selection criteria for certain type of propagating acoustic waves. If searching for Rayleigh waves then (1.41) is the only criteria to find the propagation velocity, provided the velocity search does not exceed $_{s1}$ [2, 6]. For the cases that deal with terms decaying into the depth such as longitudinal leaky waves [12], a more general method is required. For leaky SAWs the condition cannot be directly applied since the wave number (k) is complex and $\mathrm{Re}(k\alpha) \neq 0$ for all partial waves. To determine whether partial waves satisfy the radiation condition in (1.41), a small complex part is added to the velocity [8].

D. Effective Permittivity

Using (1.26) the effective permittivity can be calculated directly from kG_{44}. For the electrically open condition, the effective permittivity as a function of velocity is given as $\varepsilon_o(v)=\varepsilon_o G_o 44$, where G_{o44} is the (4,4) element of the dyadic Green's function for the electrically open condition. For the shorted condition, the effective permittivity is given as $\varepsilon_s(v)=1/(\varepsilon_o G_s 44)$, where G_{s44} is the (4,4) element of the dyadic Green's function for the electrically shorted condition. However, once the effective permittivity is computed for either the open or shorted condition the other can be easily computed by inversion (e.g. $\varepsilon_s(v) = 1/\varepsilon_o(v)$). It is convenient to express the effective permittivity as a normalized quantity, given as $\varepsilon_s(v)= \varepsilon_s(v)/\varepsilon(v=\infty)$ and $\varepsilon_o(v)= \varepsilon(v=\infty)/\varepsilon_s(v)$. To normalize, the effective permittivity is computed at a numerically large velocity. In general, the Green's functions and effective permittivity are strictly a function of k or s (i.e. slowness) since they are related in the k domain. The 4x4 dyadic Green's functions were plotted as a function of the slowness s (s/m).

IV. RESULTS

A. 128° YX Lithium Niobate (Rayleigh Waves)

The hybrid method was used to compute the Green's function 4x4 matrix for several substrates that support Rayleigh and leaky waves. To illustrate the step by step solving procedure, results are presented for 128° YX lithium niobate (LNBO) x(0°,38°,0°). The cut-off velocities were found to be 4079.17 m/s, 4793.09 m/s, and 6572.02 m/s. The roots of the eigenvalue problem were computed by solving (1.9). In Fig. 2, the real and imaginary terms of show the behavior over the velocity range. By applying the root sorting procedure discussed above, the allowed values of were selected (Fig. 3). Substitution of the selected values of into (1.33) gives a homogeneous equation, which was solved by row-reduction using each eigenvalue. The 4x4 dyadic Green's functions are shown in Fig. 4 and 5. The effective permittivity can be found from G(4,4) are discussed in section D. above.

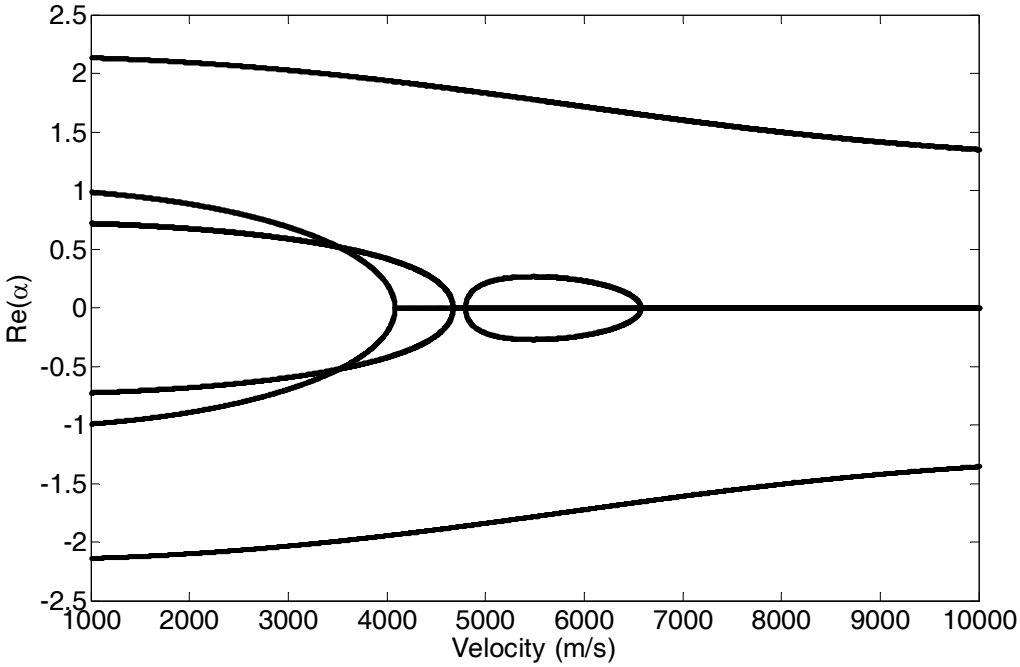

(a)

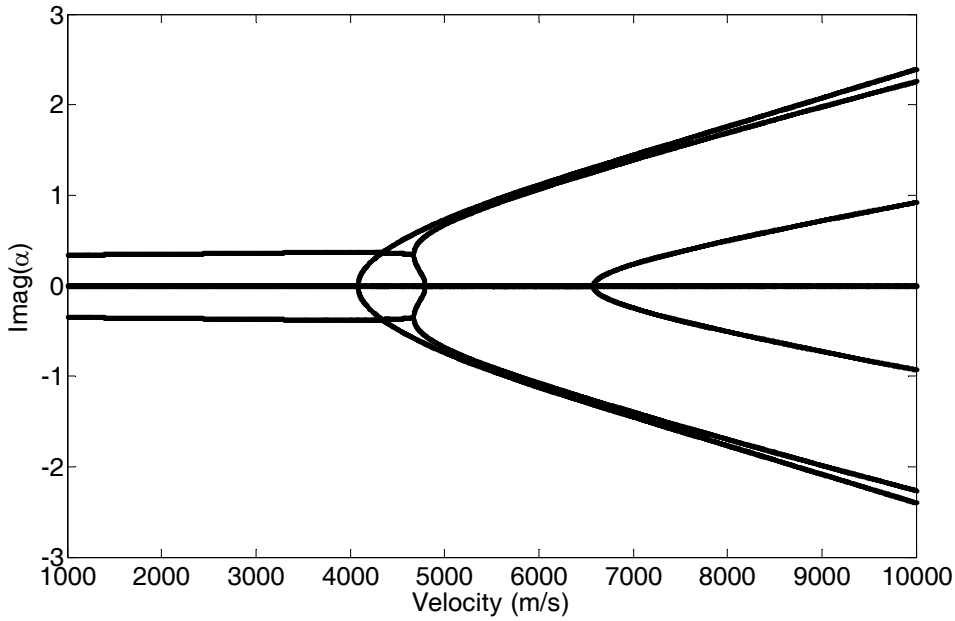

(b)

Fig. 2 Real and imaginary terms of the values of as a function of the phase velocity 128° YX LNBO. **a)** real part of and **b)** imaginary part of .

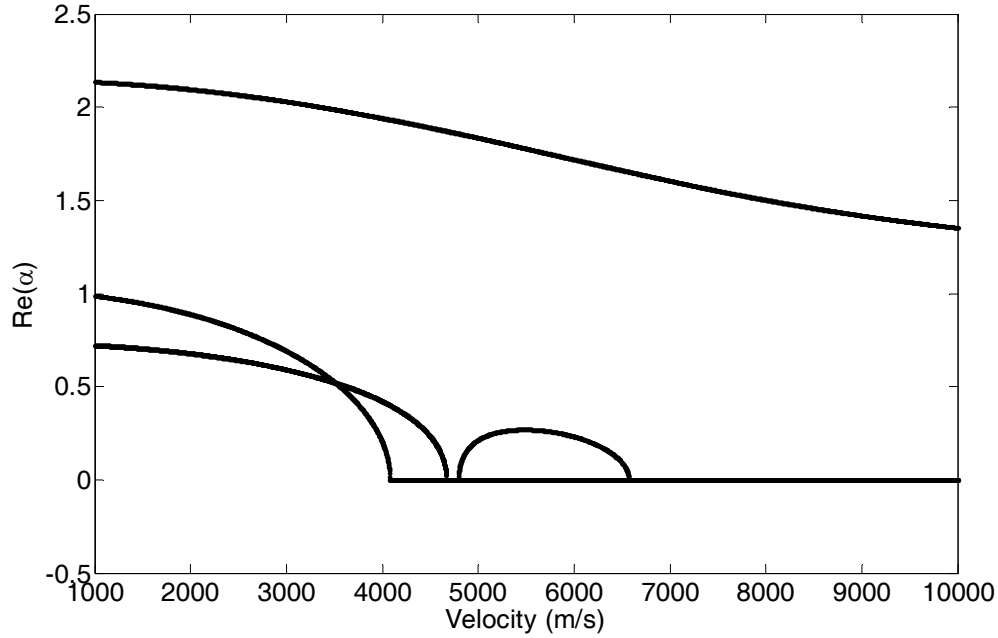

(a)

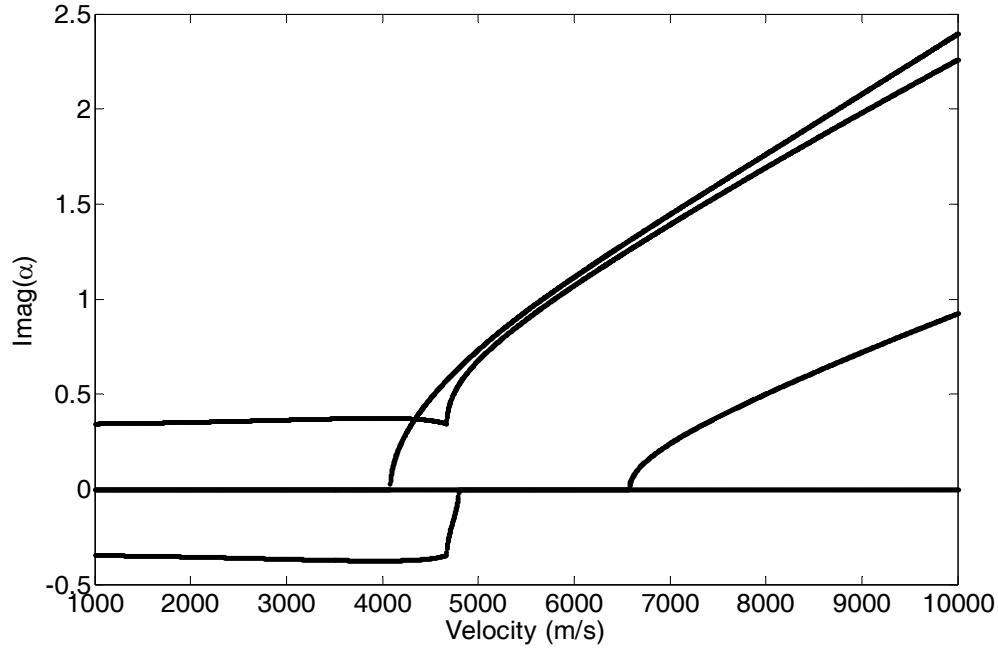

(b)

Fig. 3 Real and imaginary parts of the allowed values of as a function of the phase velocity for 128° YX LNBO. **a)** Real part of . **b)** Imaginary part of .

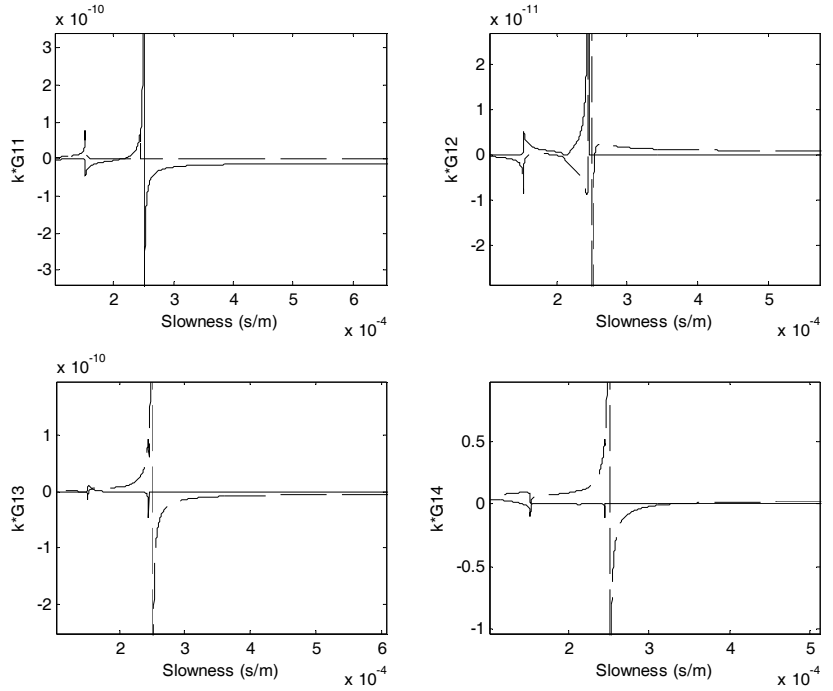

(a)

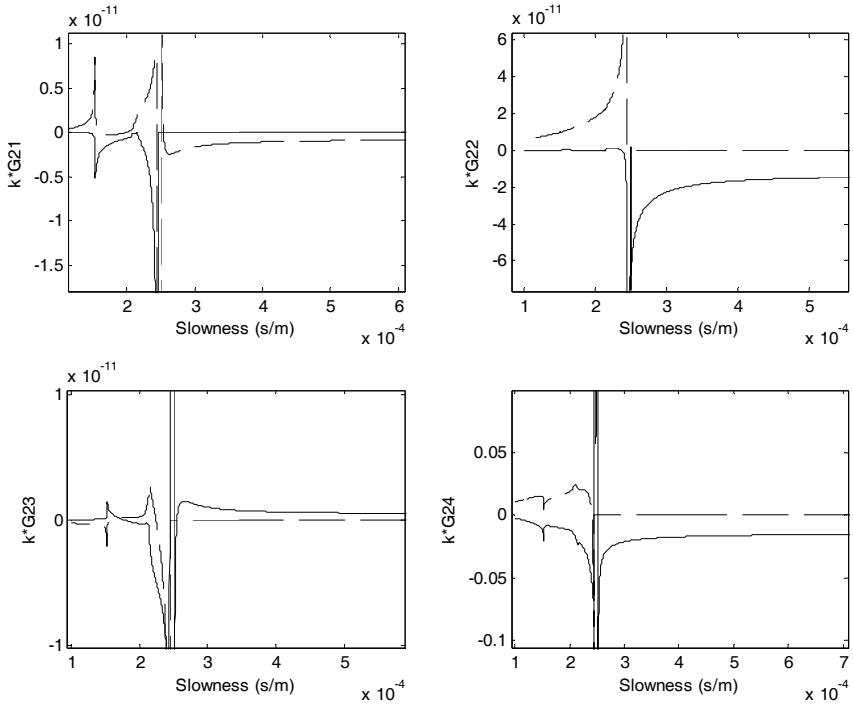

(b)

Fig. 4. Dyadic Green's function for 128° YX LNBO showing kG_{11} through kG_{24}.

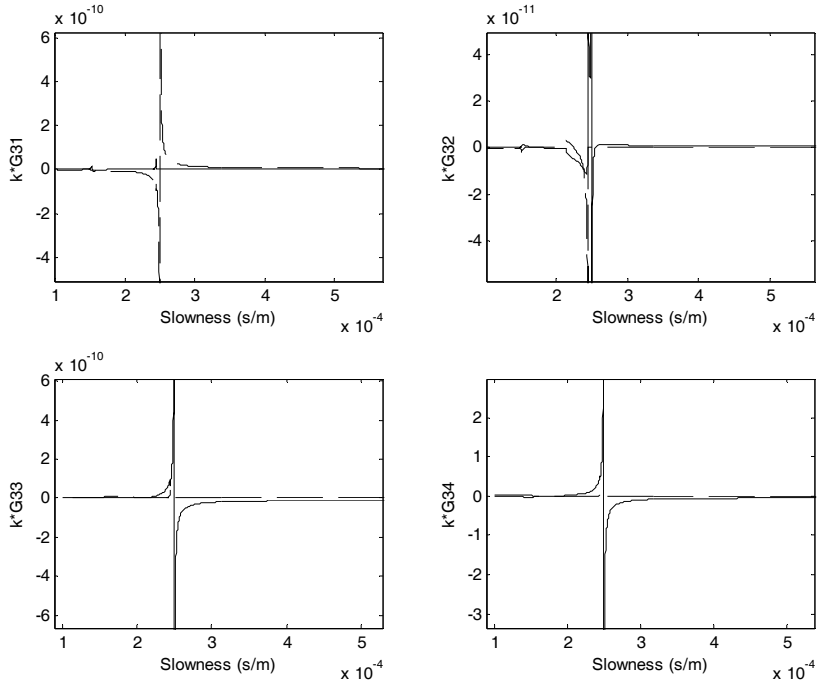

(a)

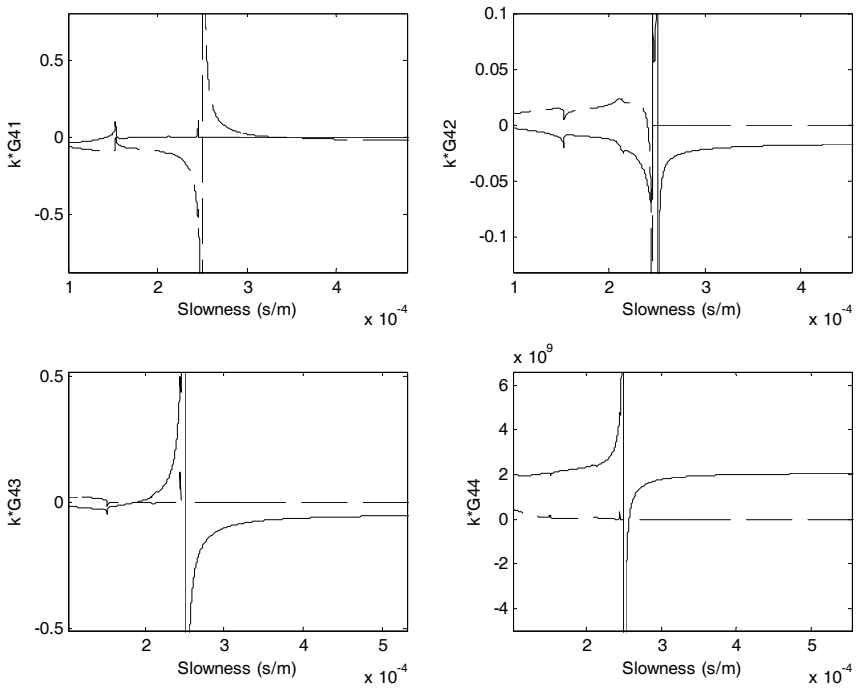

(b)

Fig. 5. Dyadic Green's function for 128° YX LNBO showing kG_{31} through kG_{44}.

B. 36° YX Lithium Tantalate (SH Leaky Waves)

For 36° YX lithium tantalate the cut-off velocities occur at 3338.1 m/s, 4171.8 m/s, and 5592.4 m/s. Using the eigenvalue selection method the proper values were chosen as shown in Fig. 6. There are three eigenvalues which lead to displacements decaying into solid with one bulk wave radiating into the solid (Fig. 6). The 4x4 dyadic Green's functions are shown in Fig. 7 and 8.

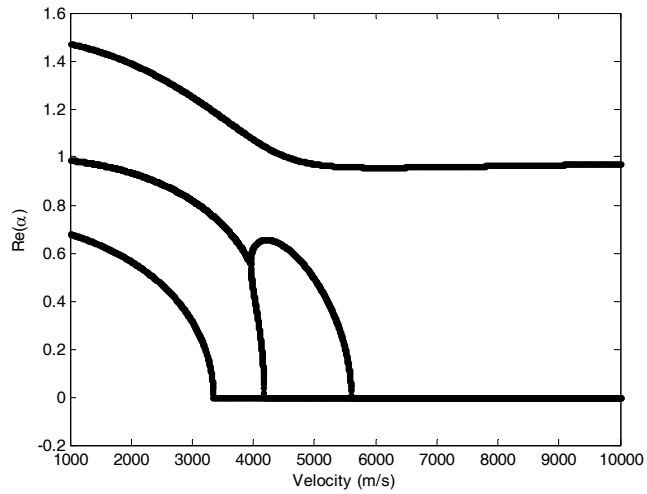

(a)

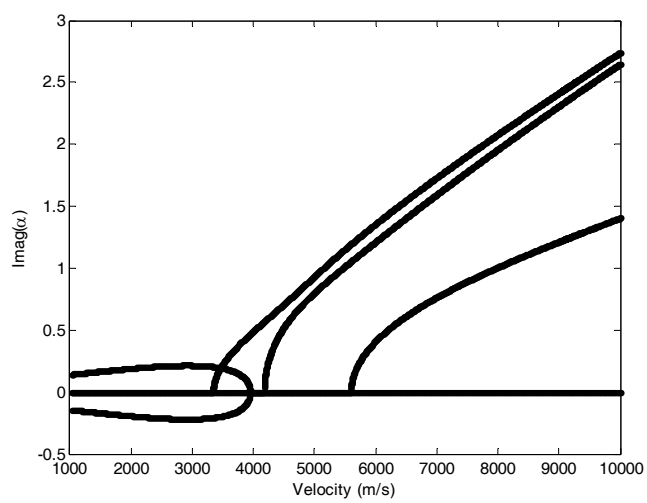

(b)

Fig. 6 Real and imaginary parts of the allowed values of as a function of the phase velocity for 36° YX LTO. **a)** Real part of . **b)** Imaginary part of .

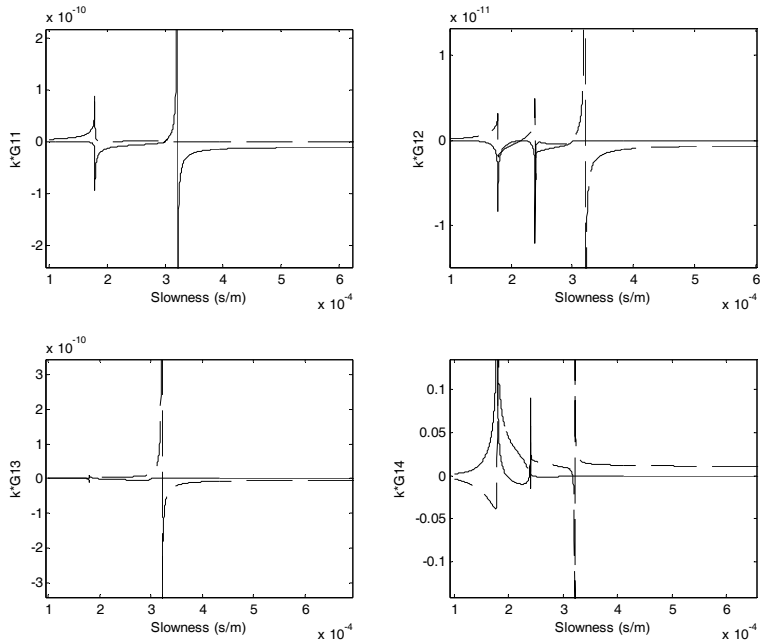

(a)

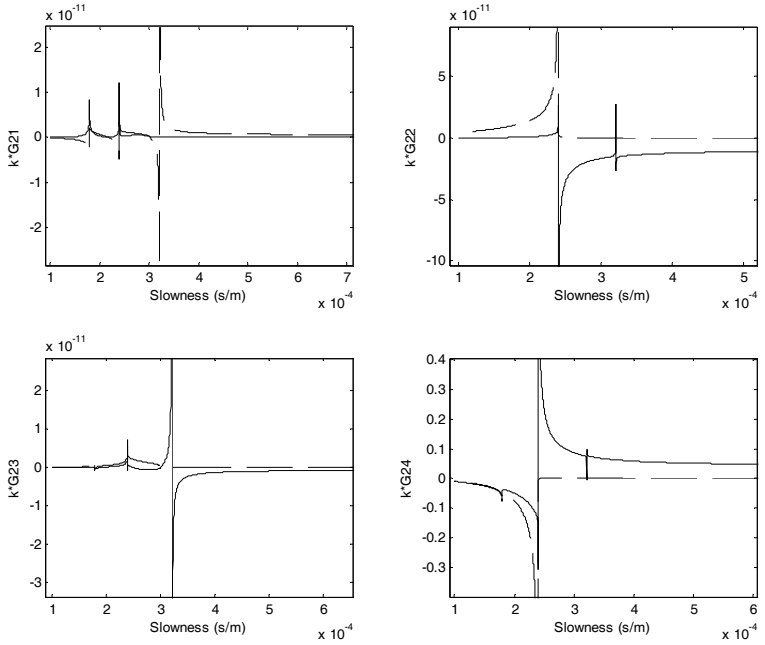

(b)

Fig. 7. Dyadic Green's function for 36° YX LTO showing kG_{11} through kG_{24}.

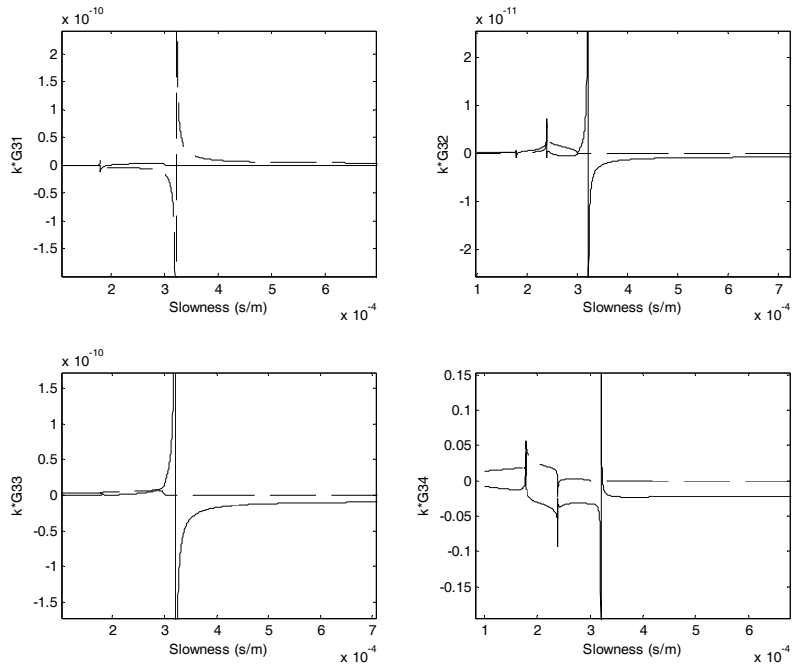

(a)

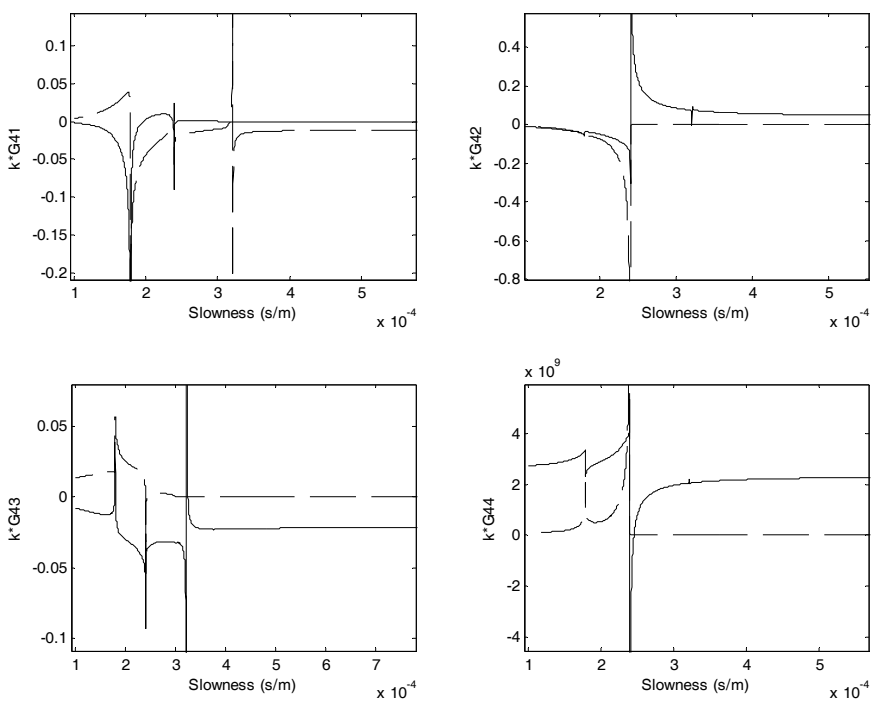

(b)

Fig. 8. Dyadic Green's function for 36° YX LTO showing kG_{31} through kG_{44}.

C. 47.3° Y 90° X off-axis Lithium Tetraborate (Longitudinal Leaky Waves)

For 47.3° Y 90° X off-axis Lithium Tetraborate (LBO) the cut-off velocities occur at 3347.1 m/s, 4556.3 m/s, and 6671 m/s. Using the eigenvalue selection method the proper values were chosen as shown in Fig. 9. In this case, longitudinal leaky waves exist in the range from $v_{s2} < v < v_l$ [12]. In this region, two bulk waves correspond to the first shear wave and second shear wave which radiate energy into the solid. The two remaining terms, the longitudinal wave the electromagnetic wave propagate along the surface decaying into the substrate. The 4x4 dyadic Green's function are shown in Fig. 10 and 11.

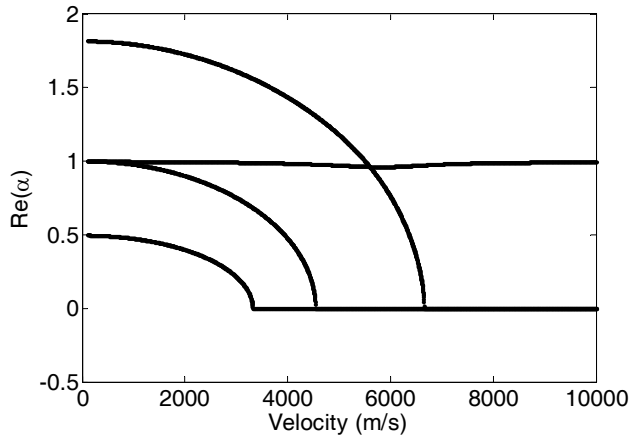

(a)

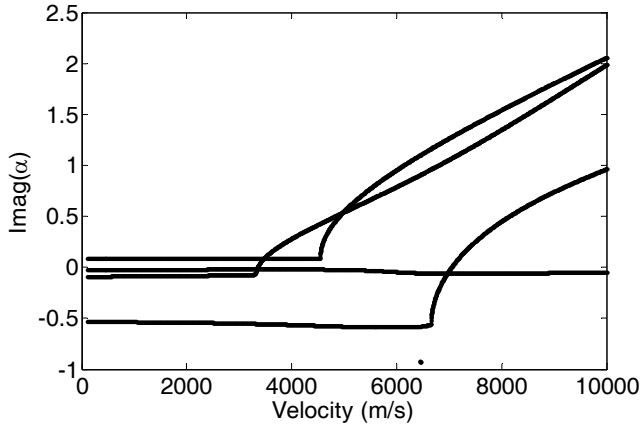

(b)

Fig. 9 Real and imaginary parts of the allowed values of as a function of the phase velocity for 47.3° Y 90° X off-axis Lithium Tetraborate (LBO). **a)** Real part of . **b)** Imaginary part of .

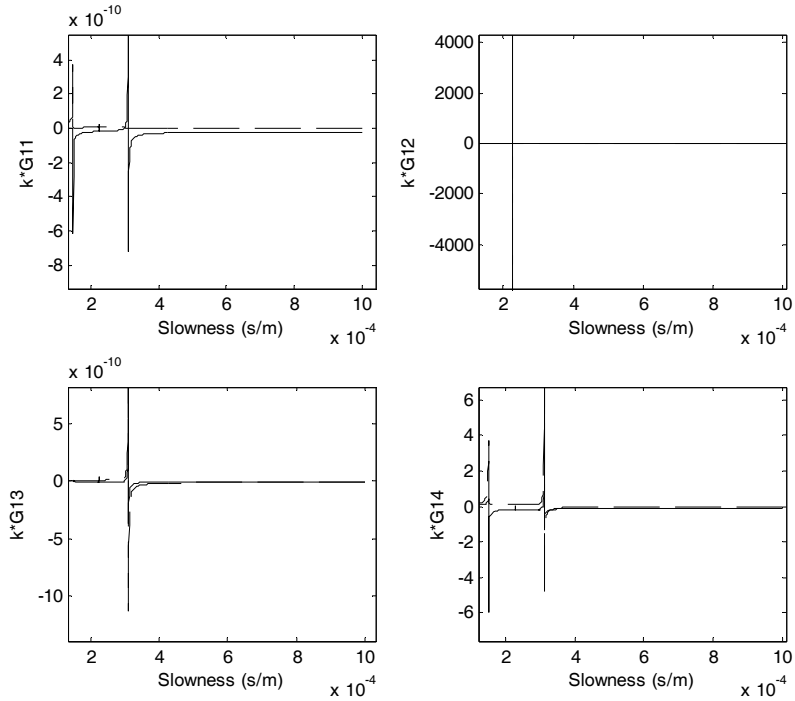

(a)

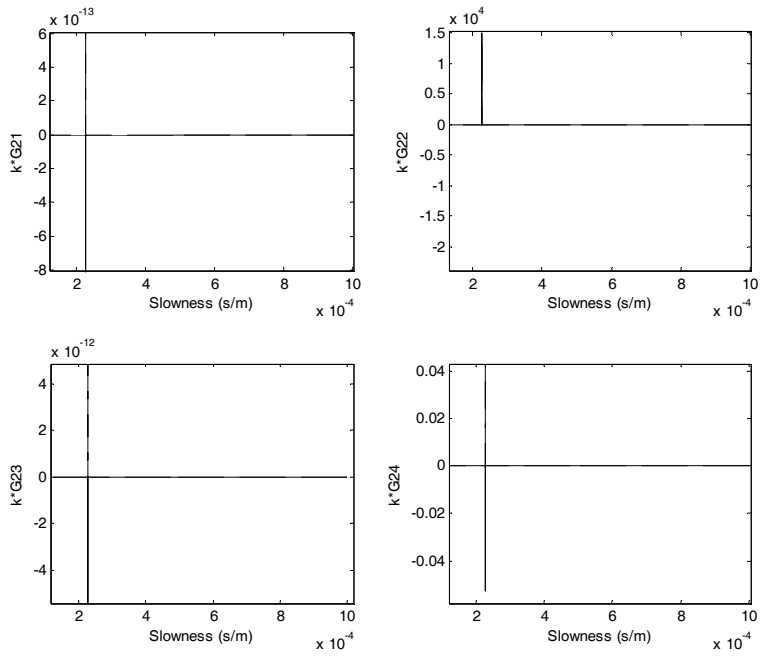

(b)

Fig. 10. Dyadic Green's function for 47.3° Y 90° X off-axis Lithium Tetraborate (LBO) showing kG_{11} through kG_{24}.

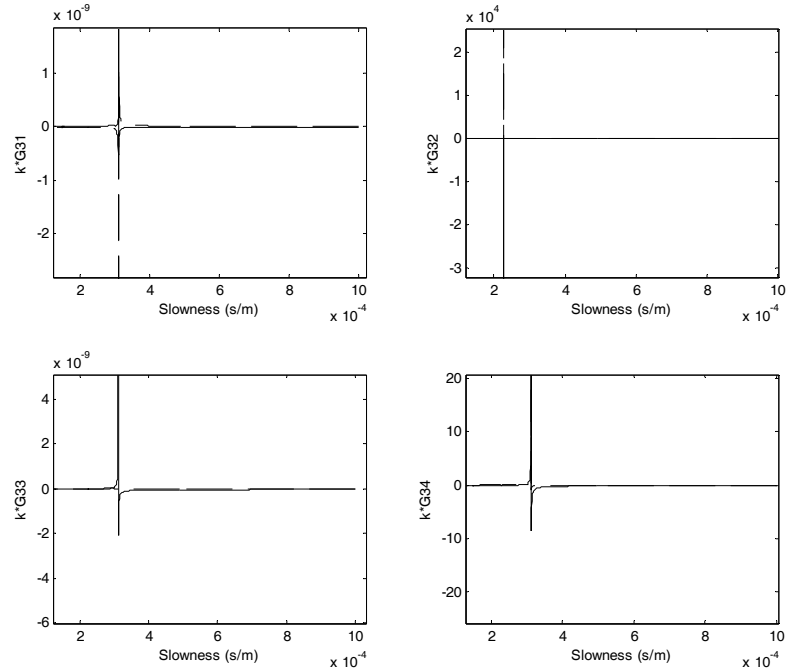

(a)

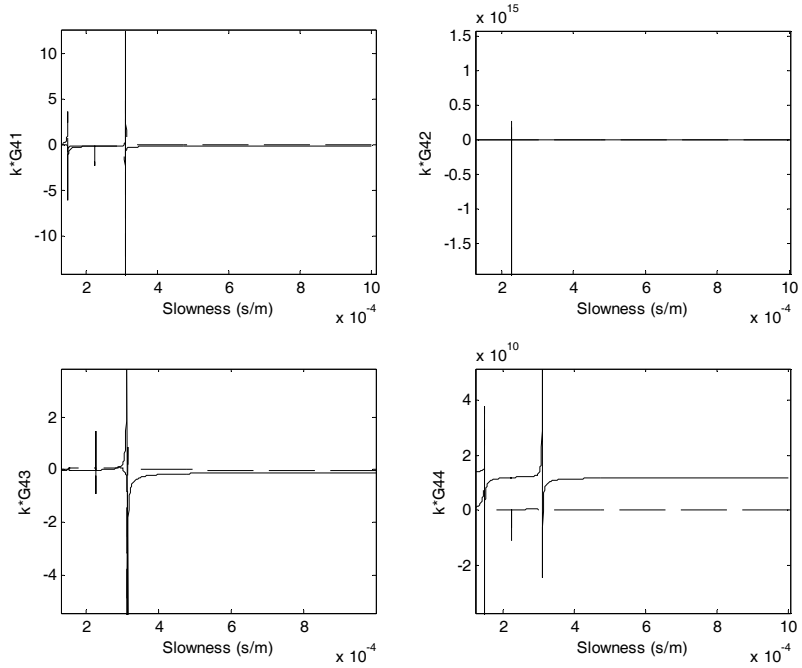

(b)

Fig. 11. Dyadic Green's function for 47.3° Y 90° X off-axis Lithium Tetraborate (LBO) showing kG_{31} through kG_{44}**.**

D. Effective Permittivity for 128º YX LNBO (SAW)

In the shorted condition (Fig. 12a) there is a pole at 3887.6 m/s. When v < 4079 the Im(ε_o) = 0) which corresponds to a true surface wave that decays into the substrate. When v > 4079 m/s, the Im(ε_o) < 0 causing bulk wave radiation into the substrate since one of the three the corresponding eigenvalues is complex with a negative imaginary part. For this substrate and cut, the wave propagation corresponds to a Rayleigh wave or RSAW at 3994.3 m/s. Though another type of RSAW exists at 3887.6 m/s, this RSAW would be highly damped by the presence a sufficiently thick metal film to achieve the shorted condition. In Fig. 12b a pole exists at 3994.3 m/s for the open condition on 128º YX LNBO (0º, 38º, 0º). Since the Im(ε_o) = 0 when v < 4079 m/s, this pole corresponds to a true surface wave that evanescently decay's into the substrate. When v > 4079 m/s the Im(ε_o) > 0 which causes waves to radiate into the substrate rather than be confined to the surface, therefore a bulk wave exists at this velocity. The SAW coupling parameter was determined to be $K^2 = 2(V_o\text{-}V_s)/V_o = 2(3994\text{-}3888)/3994 = 5.3$ %.

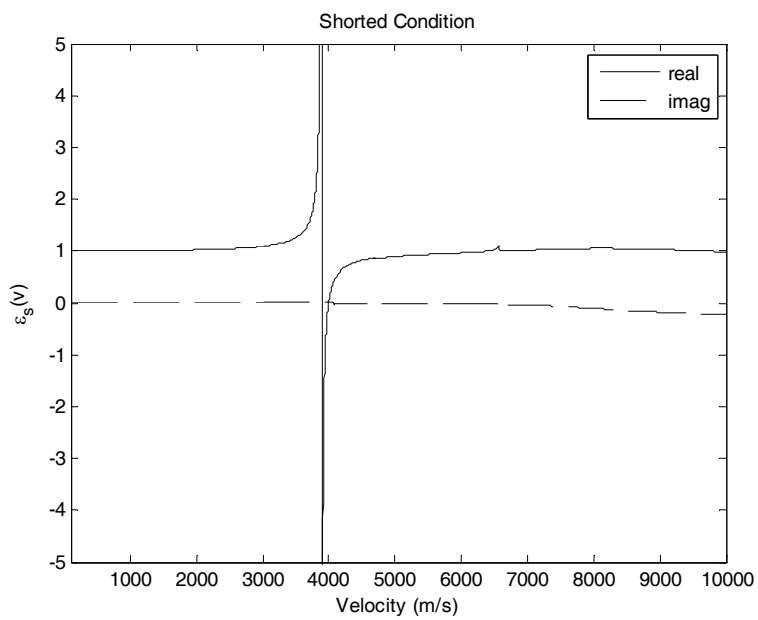

Fig. 12a The normalized effective permittivity for 128º YX LTO (0º, 38º, 0º) for the shorted condition.

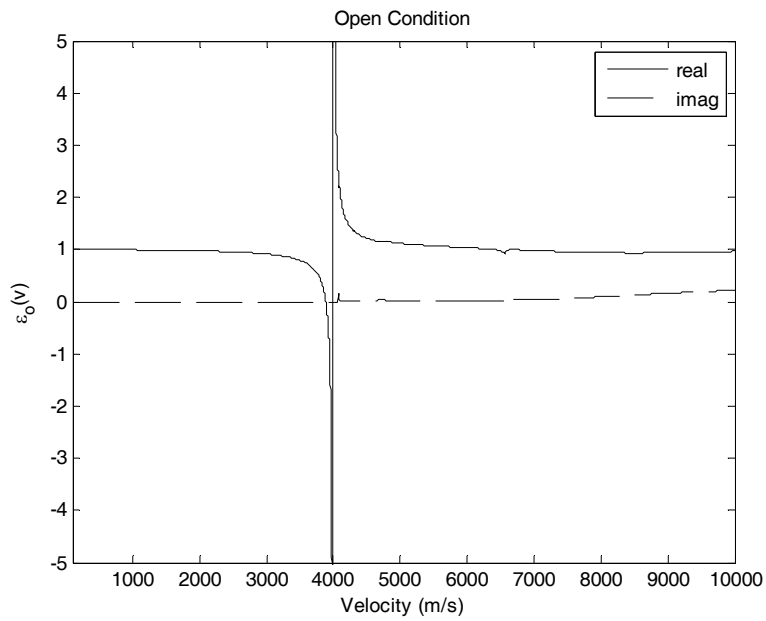

Fig. 12b The normalized effective permittivity for 128º YX LTO (0º, 38º, 0º) for open condition.

E. Effective Permittivity for 36º YX LTO (LSAW)

For the open condition a pole exists at 4171.73 m/s and for the shorted condition the pole is at 4077.06 m/s (Fig. 13a and b). The SAW coupling coefficient was computed using $K^2 = 2(V_o-V_s)/V_o$. This gives 4.5% for 36º YX LTO (0º, -54º, 0º). In the shorted condition, the $\mathrm{Im}(\varepsilon_s) < 0$ when $v < 4171$ m/s, which corresponds to partial waves decaying into the substrate. When $v > 4171$ m/s the $\mathrm{Im}(\varepsilon_s) < 0$. This causes bulk wave radiation into the substrate since one of the three the corresponding eigenvalues is complex with a negative imaginary part. In the open condition, the $\mathrm{Im}(\varepsilon_o) > 0$ when $v >$ 4171 m/s. Again the eigenvalue is complex, however with a positive imaginary part. The positive imaginary term leads to surface skimming bulk waves (SSBW) radiating into the substrate as seen by substitution of the different conditions for into (1.13). The interpretation is that for an open surface, SSBW waves dominate due to the open surface condition, and when the surface is electrically shorted, leaky SAWs (LSAW) dominate.

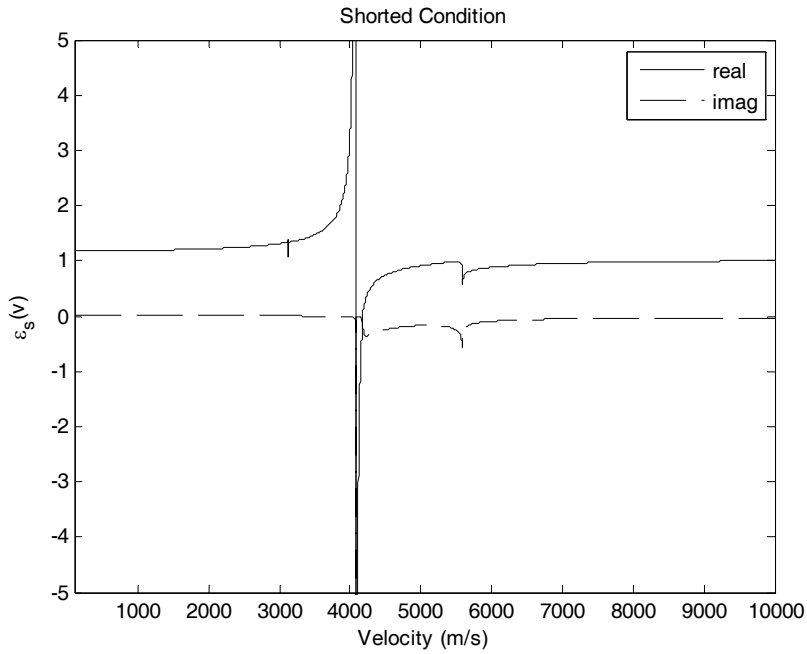

Fig. 13a The normalized effective permittivity for 36º YX LTO (0º, -54º, 0º) for the shorted condition.

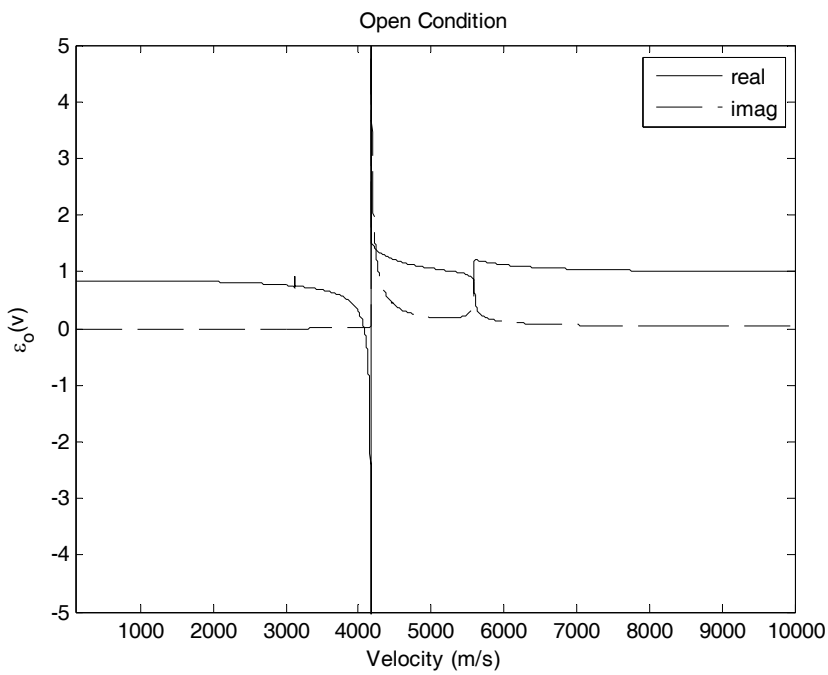

Fig. 13b The normalized effective permittivity for 36º YX LTO (0º, -54º, 0º) for the open condition.

F. Effective Permittivity for 47.3° Y 90° X off-axis Lithium Tetraborate (LLSAW)

The piezoelectric crystal lithium tetraborate (LBO) at 47.3° Y 90° X off-axis (0°, 47.3°, 90°) supports longitudinal leaky waves or LLSAWs. The pole located at 3205 m/s represents a Rayleigh SAW when the surface is shorted (Fig. 14a). The Im(ε_s) = 0 when v < 3316 m/s which causes all the partial waves to be evanescent into the substrate therefore the pole at 3205 represents a true surface wave. When v > 3316 m/s, the Im(ε_s) < 0, causing the partial waves to radiate energy into the substrate. A secondary pole exists at 6614 m/s with a symmetrical imaginary part causing energy to leak into the substrate which is the LSAW. In Fig. 14b when v > 6660 m/s the Im(ε_s) > 0 with an asymmetrical imaginary term. This suggests the presence of a SSBW radiating into the substrate. Of significance is that by shorting the surface through application of a metal film, the high velocity SSBWs can be converted to LLSAW waves.

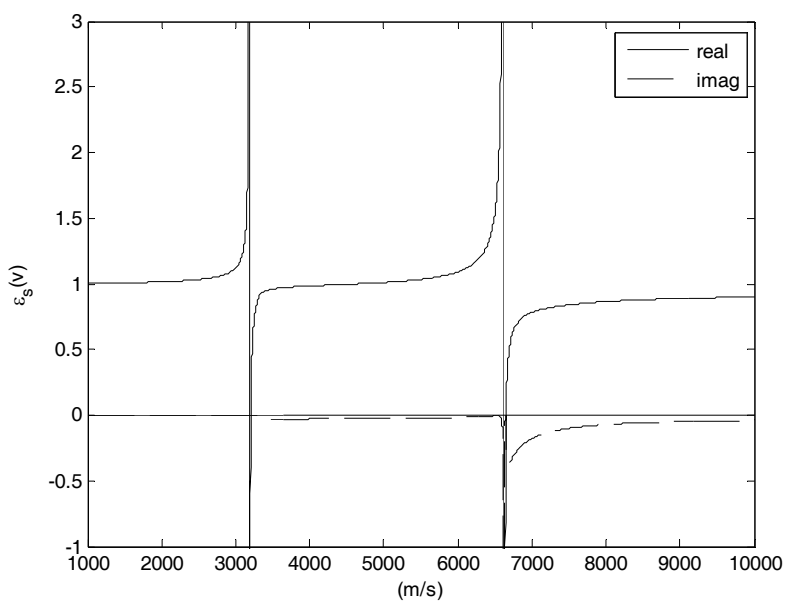

Fig. 14a The normalized effective permittivity for 47.3° Y 90° X off-axis LBO (0°,47.3°,90°) for the shorted condition.

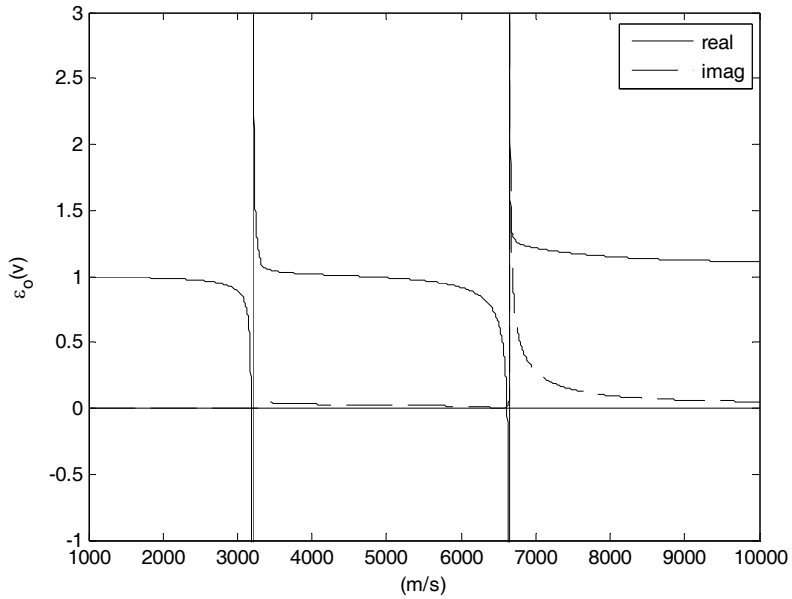

Fig. 14b The normalized effective permittivity for 47.3° Y 90° X off-axis LBO (0°,47.3°,90°) for the open condition.

CONCLUSIONS

To facilitate analysis of SAW devices and interdigital transducer design, an alternate method for computing the dyadic Green's functions has been developed. In this method, the eigenvalues are determined from an eighth order polynomial formed by assuming plane wave solutions in the substrate and overlying films. A selection criterion was developed to automatically determine the allowed eigenvalues for any type of wave propagation. Using the four allowed eigenvalues, the general eigenvalue problem was rewritten to permit solving for each corresponding eigenvector separately. These eigenvectors give the corresponding stresses, electric displacement, displacement, and the electric potential in the substrate. Three substrates were used to demonstrate this method which supported RSAW, LSAW, and LLSAW behavior. The G_{44} element was used to determine the effective permittivity which relates the surface charge to the surface potential. The existence of poles in the effective permittivity analysis determines the location of surface waves, bulk waves, and their corresponding behavior.

REFERENCES

[1] K. A. Ingebrigtsen, "Surface-acoustic waves in piezoelectrics," *J. Appl. Phys.*, vol. 40, pp. 2681-2686, 1969.

[2] J. J. Campbell and W. R. Jones, "A method for estimating optimal crystal cuts and propagation directions for excitation of piezoelectric surface waves," *IEEE Trans. Sonics Ultrason.*, vol. 15, pp. 209-217, 1968.

[3] E. L. Adler, "SAW and pseudo-SAW properties using matrix methods," *IEEE Trans. Ultrason. Ferroelectr. Freq. Cntrl*, vol. 41, pp. 876-882, 1994.

[4] R. C. Peach, "A general Green's function analysis for SAW devices," *IEEE Ultrason. Symp. Proc.*, pp. 221-225, 1995.

[5] V. P. Plessky and T. Thorvaldsson, "Periodic Green's functions analysis of SAW and leaky propagation in a periodic system of electrodes on a piezoelectric crystal," *IEEE Trans. Ultrason., Ferroelectr. Freq. Cntrl.*, vol. 42, pp. 280-293, 1995.

[6] J. J. Campbell and W. R. Jones, "Propagation of surface waves at the boundary between a piezoelectric crystal and a fluid medium," *IEEE Trans. Sonic and Ultrason.*, vol. 17, pp. 71-76, 1970.

[7] G. W. Farnell, "Symmetry considerations for elastic layer modes propagating in anisotropic piezoelectric crystals," *IEEE Trans. Son. Ultrason.*, vol. 17, pp. 229-238, 1970.

[8] K. Y. Hashimoto, *Surface acoustic wave devices in telecommunications: Modeling and Simulation*. Berlin: Springer-Verlag, 2000.

[9] D. Qiao, W. Liu, and P. M. Smith, "General Green's functions for SAW device analysis," *IEEE Trans. Ultrason. Ferroelectr. Freq. Cntrl*, vol. 46, pp. 1242-1253, 1999.

[10] B. A. Auld, *Acoustic fields and waves in solids*, 2nd ed. ed. Malabar: Krieger Publishing Co., 1990.

[11] T. C. Lim and G. W. Farnell, "Character of pseudo surface waves on anisotropic crystals," *J. Acoust. Soc. Amer.*, vol. 45, pp. 845-851, 1969.

[12] T. Sato and H. Abe, "Propagation properties of longitudinal leaky surface waves on lithium tetraborate," *IEEE Trans. Ultrason. Ferroelectr. Freq. Cntrl*, vol. 45, pp. 136-151, 1998.

DISTRIBUTION LIST

10	MS 1425	Darren W. Branch
1	MS 0892	Thayne Edwards
2	MS 1425	Steve Casalnuovo
1	MS 0892	Richard Cernosek
1	MS 0899	Technical Library, 9536